

Optomechanical Two-Photon Hopping

Enrico Russo,^{1,*} Alberto Mercurio,¹ Fabio Mauceri,¹ Rosario Lo Franco,² Franco Nori,^{3,4,5} Salvatore Savasta,^{1,3} and Vincenzo Macri^{3,2,†}

¹*Dipartimento di Scienze Matematiche e Informatiche,*

Scienze Fisiche e Scienze della Terra, Università di Messina, I-98166 Messina, Italy

²*Dipartimento di Ingegneria, Università degli Studi di Palermo, Viale delle Scienze, 90128 Palermo, Italy*

³*Theoretical Quantum Physics Laboratory, RIKEN, Wako-shi, Saitama 351-0198, Japan*

⁴*RIKEN Center for Quantum Computing (RQC), Wako-shi, Saitama 351-0198, Japan*

⁵*Physics Department, The University of Michigan, Ann Arbor, Michigan 48109-1040, USA*

(Dated: August 12, 2022)

The hopping mechanism plays a key role in collective phenomena emerging in many-body physics. The ability to create and control systems that display this feature is important for next generation quantum technologies. Here we study two cavities separated by a vibrating two-sided perfect mirror and show that, within currently available experimental parameters, this system displays photon-pair hopping between the two electromagnetic resonators. In particular, the two-photon hopping is not due to tunneling, but rather to higher-order resonant processes. Starting from the classical problem, where the vibrating mirror perfectly separates the two sides of the cavity, we quantize the system and then the two sides can interact. This opens the possibility to investigate a new mechanism of photon-pair propagation in optomechanical lattices.

The mastery of manipulating quantum mechanical systems by means of radiation pressure has opened the door to fundamental tests of quantum theory [1, 2], to precision measurements [3–5] and to novel quantum technologies [6–8]. For instance, laser cooling techniques [9–11] allow to observe quantized vibrational modes of macroscopic objects and even the possibility to reach their ground-state [12–14]. This has paved the way to the realisation of entangled macroscopic states and, in turn, new ways to process and store quantum information [15–18]. Notably, with these techniques optomechanical crystals [19–21] can be scaled to form optomechanical arrays where, using hopping mechanisms, applications for quantum information processing have been proposed [22, 23].

Cavity-optomechanics, in particular, lies at the crossroad of wide research lines that are currently under active investigation. In experiments [8, 17, 24, 25], only radiation pressure effects have been considered, as the cavity frequencies far outweigh the mirror ones. On the other hand, ultra-high-frequency mechanical oscillators [26, 27] coupled to microwave ones offer the potential to observe, for instance, dynamical Casimir effects [28–33]. The case of one such mirror interacting with a single cavity mode was first considered in Ref. [34], and this study was later extended to include an incoherent excitation of the mirror [35–37]. In the same setup, back-reaction and dissipation effects have also been studied [38, 39]. Finally, the case of a cavity with two moving walls was addressed [40, 41]; in this case, the cavity field mediates an effective interaction between the two mirrors leading to a phonon hopping.

A suitable platform to experimentally reproduce these predictions is circuit optomechanics. In fact, the addition of artificial atoms in a superconducting microwave

setup strengthens the coupling with the mechanical resonator [27, 42, 43], and introducing high-frequency mirrors makes it a very promising setup. A valuable alternative would be to use a quantum simulator [44, 45] where two *LC* circuits replace the two cavities, and a superconducting quantum interference device (SQUID) is deployed instead of the high-frequency vibrating mirror.

The availability of these experimental platforms led us to design a system that, under certain resonance conditions, allows for a simultaneous hopping of photon-pairs. The system consists of two non-interacting electromagnetic resonators separated by a movable two-sided perfect mirror. The vibrational modes of the mirror act as a mediator between the two resonators, making the photon-pair hopping possible. The vibrating mirror separates both sides of the cavity at the classical level, but not quantum mechanically. Our Hamiltonian is obtained quantizing the classical problem, generalizing the results in Ref. [46]. It accounts also for generic equilibrium po-

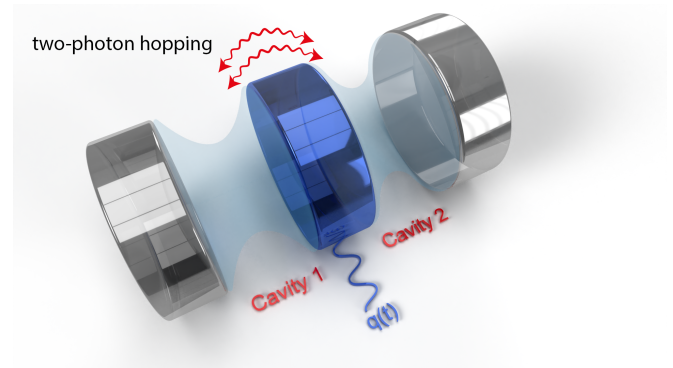


FIG. 1. Proposal sketch. Two non-interacting electromagnetic cavities separated by a movable two-sided perfect mirror.

* enricorussoxvi@gmail.com

† vincenzo.macri@riken.jp

sitions of the mirror even though, in what follows, we consider only the symmetric case.

Similar setups have been studied, for instance, in Ref. [47] where the authors analyzed the dressing of the ground state and the correlation functions between the two separated regions, and in Ref. [48] where the two resonators are separated by a dielectric. In our treatment the two-photon hopping mechanism appears as a spontaneous coherent process in a second-order effective dynamics. Note that the optomechanical hopping described here does not involve photon tunneling, which is the usual photon hopping mechanism studied elsewhere. Our interest in these hopping effects stems from the possibility to envision optomechanical lattices, with unit cells as in Fig. 1, and to study their thermodynamic and information properties. Thus, extended optomechanical lattices would display an interesting interplay between the Casimir photon-pairs creation and the lattice inter-site hopping.

RESULTS

The quantum model. Consider two non-interacting electromagnetic cavities separated by a vibrating two-sided perfect mirror as sketched in Fig. 1. Following Ref. [46] we quantized (see Methods) the classical system obtaining the Hamiltonian ($\hbar = 1$)

$$\hat{H} = \omega_a \hat{a}^\dagger \hat{a} + \omega_b \hat{b}^\dagger \hat{b} + \omega_c \hat{c}^\dagger \hat{c} + \frac{g}{2} \left[(\hat{c} + \hat{c}^\dagger)^2 - \left(\frac{\omega_a}{\omega_c} \right)^2 (\hat{a} + \hat{a}^\dagger)^2 \right] (\hat{b} + \hat{b}^\dagger). \quad (1)$$

Here, \hat{b} (\hat{b}^\dagger) is the creation (annihilation) operator of the moving mirror, \hat{a} (\hat{a}^\dagger) and \hat{c} (\hat{c}^\dagger) are the creation (annihilation) operators of the left and right cavity, respectively. The parameters ω_a , ω_b and ω_c are the corresponding bare energies of the three boson modes. The coupling strength $g = \omega_c^2 x_{z\text{zpf}} / \pi$ depends both on the zero-point-fluctuation amplitude of the mirror $x_{z\text{zpf}}$, and on the bare energy of a cavity ω_c , taken for convenience as the right one. The weight ω_a^2 / ω_c^2 accounts for asymmetrical configurations. The linear approximation implicit in Eq. (1) does not lead to instabilities of the ground state as long as $g\omega_a < \omega_c^2$, i.e., $\omega_a x_{z\text{zpf}} < \pi$. The sought-after hopping mechanism occurs at the resonance $\omega_a = \omega_c$. We consider the case when the bare frequency of the mirror is lower than the cavity frequency. This choice of parameters identifies a set of avoided-level crossings in the Hamiltonian spectrum, and thus a particular closed sub-dynamics, as can be seen from Fig. 2,

Figure 2(a) shows the lowest energy levels obtained by numerically diagonalising the full Hamiltonian Eq. (1) (blue dashdotted curves), while Fig. 2(b) is an enlarged view of the avoided-level crossing inside the black rectangle. The gap is a trademark of the hybridization of the two states $|\psi_1\rangle$ and $|\psi_2\rangle$, eigenstates of the full Hamiltonian Eq. (1). A local effective description (red dashed

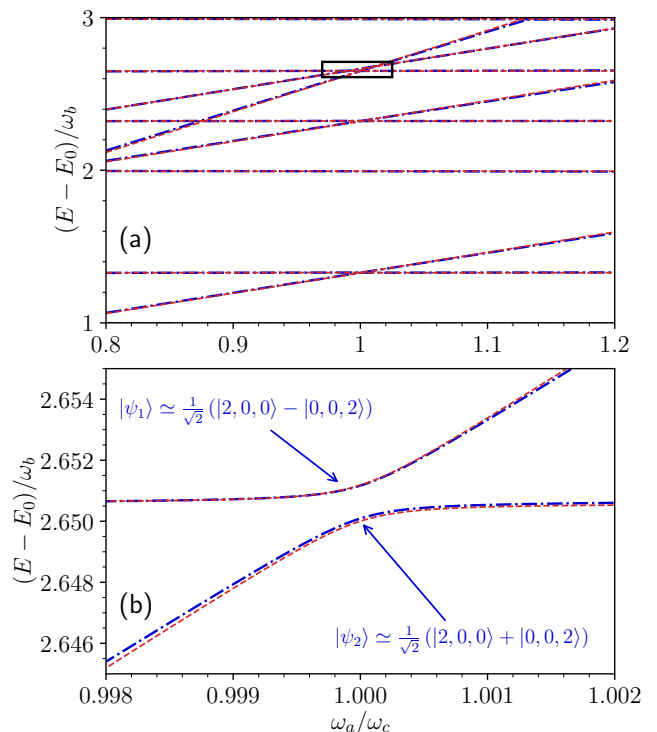


FIG. 2. (a) The lowest energy levels of the system Hamiltonian versus the ratio between the two cavity frequencies. For a coupling $g = 0.06 \omega_b$, the position of the avoided level crossing is contained in the black rectangle. (b) An enlarged view of the latter is given. The presence of the labels stress the hybridisation of the two states $|2, 0, 0\rangle$ and $|0, 0, 2\rangle$. The frequency mirror was conveniently set as $\omega_b = 3/4 \omega_c$.

curves) is possible through the generalized James' effective approach [49] (see Methods), with resonance conditions $\omega_c = \omega_a$

$$\begin{aligned} \hat{H}_{\text{eff}}^{(2)} &= \hat{H}_{\text{shift}}^{(2)} + \hat{H}_{\text{hop}}^{(2)}, \\ \hat{H}_{\text{shift}}^{(2)} &= \left[\omega_a + \frac{g^2(4\omega_a + \omega_b)}{8\omega_a^2 - 2\omega_b^2} \right] (\hat{c}^\dagger \hat{c} + \hat{a}^\dagger \hat{a}) \\ &\quad + \frac{g^2(3\omega_b^2 - 8\omega_a^2)}{(8\omega_a^2 - 2\omega_b^2)\omega_b} [(\hat{c}^\dagger \hat{c})^2 + (\hat{a}^\dagger \hat{a})^2] \\ &\quad + \left[\omega_b + \frac{4g^2\omega_a}{4\omega_a^2 - \omega_b^2} (\hat{a}^\dagger \hat{a} + \hat{c}^\dagger \hat{c} + \mathbf{1}) \right] \hat{b}^\dagger \hat{b} \\ &\quad + \frac{2g^2}{\omega_b} \hat{a}^\dagger \hat{a} \hat{c}^\dagger \hat{c} + \frac{g^2}{2\omega_a - \omega_b} \mathbf{1}, \\ \hat{H}_{\text{hop}}^{(2)} &= -\frac{g^2\omega_b}{8\omega_a^2 - 2\omega_b^2} (\hat{a}^2 \hat{c}^{\dagger 2} + \hat{a}^{\dagger 2} \hat{c}^2). \end{aligned} \quad (2)$$

The first term, $\hat{H}_{\text{shift}}^{(2)}$, contains the bare Hamiltonians and both cross- and self-Kerr non-linearities. The second term, $\hat{H}_{\text{hop}}^{(2)}$ is the one responsible for the two-photon hopping. Since $[\hat{a}^\dagger \hat{a}, \hat{H}_{\text{shift}}^{(2)}] = [\hat{b}^\dagger \hat{b}, \hat{H}_{\text{shift}}^{(2)}] = [\hat{c}^\dagger \hat{c}, \hat{H}_{\text{shift}}^{(2)}] = 0$ we can still choose as an unperturbed base the states $|n_a, n_b, n_c\rangle$, where n_a (n_c) is the number of photon in

the left (right) cavity, and n_b the number of phonons in between; all of these three are considered with shifted energies due to interaction with the fields.

Analytical aspects. The two states $|\psi_{1,2}\rangle = (|2, 0, 0\rangle \pm |0, 0, 2\rangle)/\sqrt{2}$ are eigenstates of the full (effective) Hamiltonian. To have a simple analytical description, we limit our analysis to the subspace spanned by $\{|2, 0, 0\rangle, |0, 0, 2\rangle\}$ around the avoided-level crossing. If we initialise the system in either $|2, 0, 0\rangle$ or $|0, 0, 2\rangle$, we witness a coherent oscillatory dynamics between the two maximally entangled photon-pair states. Neglecting dressing energy shifts, which have been reabsorbed by an appropriate choice of the coefficients, the effective interaction Hamiltonian $\hat{H}_{\text{hop}}^{(2)}$ in Eq. (2) can be used to solve the stochastic evolution of the system wave function (see Methods). By projecting the time-evolution operator $\hat{U}(t) = \exp(-i\hat{\mathcal{H}}t)$ onto the $2D$ subspace $\{|2, 0, 0\rangle, |0, 0, 2\rangle\}$, with

$$\hat{\mathcal{H}} = \hat{H}_{\text{hop}}^{(2)} - i(\gamma_a \hat{a}^\dagger \hat{a} + \gamma_b \hat{b}^\dagger \hat{b} + \gamma_c \hat{c}^\dagger \hat{c})/2, \quad (3)$$

in the interaction picture we obtain

$$\hat{U}(t) = e^{-2\gamma t} [\cos(\tilde{g}t) (|2, 0, 0\rangle \langle 2, 0, 0| + |0, 0, 2\rangle \langle 0, 0, 2|) - i \sin(\tilde{g}t) (|2, 0, 0\rangle \langle 0, 0, 2| + |0, 0, 2\rangle \langle 2, 0, 0|)], \quad (4)$$

where we choose $\gamma = \gamma_a = \gamma_c$ and $\tilde{g} = g^2 \omega_b / 2(4\omega_a^2 - \omega_b^2)$. If we initialize the system in the state $|2, 0, 0\rangle$, its evolution at time t , before a quantum jump takes place, is

$$|\psi(t)\rangle = e^{-2\gamma t} [\cos(\tilde{g}t) |2, 0, 0\rangle - i \sin(\tilde{g}t) |0, 0, 2\rangle]. \quad (5)$$

By appropriately renormalizing the wave function, we obtain the mean photon number for the left and right cavities and for the mechanical resonator

$$\begin{aligned} \langle \hat{a}^\dagger \hat{a} \rangle &= 2 \cos^2(\tilde{g}t), \\ \langle \hat{b}^\dagger \hat{b} \rangle &= 0, \\ \langle \hat{c}^\dagger \hat{c} \rangle &= 2 \sin^2(\tilde{g}t). \end{aligned} \quad (6)$$

The expectation values on a single quantum trajectory for a generic operator \hat{O} is denoted as $\langle \hat{O}(t) \rangle$, while average quantities obtained over an ideally infinite number of quantum trajectories are indicated as $\langle \hat{O}(t) \rangle$.

Numerical results. Figure 3(a) shows an example of a single quantum trajectory, obtained by solving numerically the stochastic evolution of the system wave function. It shows the time evolution of the mean photon number $\langle \hat{a}^\dagger \hat{a} \rangle$ (blue curve), $\langle \hat{c}^\dagger \hat{c} \rangle$ (black dashdotted curve), of the left and right cavity respectively, and the phonon number $\langle \hat{b}^\dagger \hat{b} \rangle$ (red dashed curve). The system is initialized in the state $|2, 0, 0\rangle$, as in the analytical case. Before a quantum jump occurs, the numerical simulation displays the oscillation predicted by Eq. (6). When the

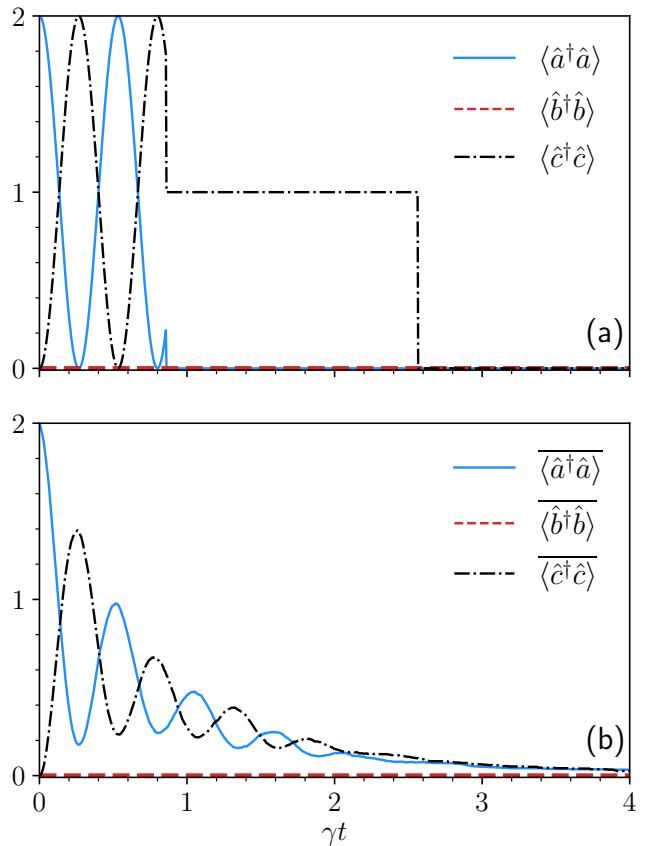


FIG. 3. Panel (a) shows an example of a single quantum trajectory, numerically obtained by studying the open quantum dynamics. It shows the time evolution of the mean photon number of the left cavity $\langle \hat{a}^\dagger \hat{a} \rangle$ (blue curve), right cavity $\langle \hat{c}^\dagger \hat{c} \rangle$ (black dashdotted curve) and of the phonon number of the movable mirror $\langle \hat{b}^\dagger \hat{b} \rangle$ (red dashed curve). The system is initialized in $|2, 0, 0\rangle$ at the resonant condition $\omega_c = \omega_a$, and $\omega_b = 3\omega_a/4$. The numerical simulation initially displays the oscillation predicted by Eq. (5) until a quantum jump occurs in the right cavity. The measure collapse the state into $-i|0, 0, 1\rangle$. Even though the two cavities are in resonance, the state $|0, 0, 1\rangle$ is locked: the photon remains confined in the right cavity. This is an optomechanical feature of our system. After the second jump occurs, the system reaches the state $|0, 0, 0\rangle$. In panel (b) an average over 500 trajectories is shown. Clearly, there is a coherent evolution of two photon-pairs state. Such results can be attained as well with a master equation approach, but the locking feature is lost in the average. In both panels, the parameters are $g = 0.06\omega_b$, $\omega_a = \omega_c = 4\omega_b/3$, and $\gamma_a = \gamma_b = \gamma_c = \gamma = 10^{-4}\omega_b$.

right detector clicks, one photon has escaped from the right cavity. Therefore, the state in Eq. (5) collapses to $-i|0, 0, 1\rangle = \hat{c}|\psi(t)\rangle / [\langle \psi(t) | \hat{c}^\dagger \hat{c} | \psi(t) \rangle]^{1/2}$. This state is preserved until a second jump occurs, i.e., the photon remains locked in the right cavity. This is an optomechanical feature of our system. Indeed, the absence of linear interaction terms in Eq. (2) denies a one-to-one conversion among the subsystems. Hence, when the second photon jump occurs, it is certain that the state collapses to $|0, 0, 0\rangle = \hat{c}|0, 0, 1\rangle$.

In Fig. 3(b) the dynamics is shown averaged over 500 trajectories. Clearly, we see a coherent oscillation of a

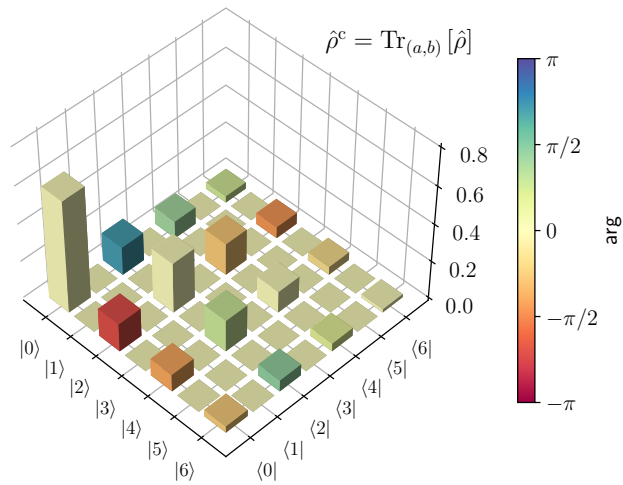


FIG. 4. Density matrix elements of the right cavity. It is obtained partially tracing over the left cavity and the mirror. Only *even number states* are filled when the right cavity is initially empty and a coherent incoming pulse enters the left cavity. This is in full agreement with the hopping mechanism we proposed. The parameters used here are $g = 0.09\omega_b$, $\omega_a = \omega_c = 1.1\omega_b$, and $\gamma_a = \gamma_b = \gamma_c = 0$.

photon-pair. Of course, in presence of decoherence, such result can be obtained also adopting a master equation approach, but the locking feature emerges only under a post-selection procedure or by studying a single quantum trajectory [50, 51]. Note that, with the parameters used we obtain an effective coupling $\tilde{g} \approx 3 \times 10^{-4}\omega_b$, which is almost three times greater than the loss rate γ (the latter related to the cavity quality factor Q). This regime, defined as strong coupling, allows the photon pairs to flow from one cavity to the other for a certain time before one photon is lost to the environment.

We conclude this work considering the case of an incoming Gaussian coherent pulse driving the left cavity while the system is initially in its ground state. For simplicity we present a numerical simulation for the closed dynamics. Figure 4 shows the first matrix elements of the density operator at the end of the dynamics. The state of the right cavity contains only even occupation numbers: in a closed dynamics no loss is possible and the hopping mechanism always involves photon pairs.

DISCUSSION

We have carried out a theoretical analysis of an optomechanical system consisting of two electromagnetic resonators separated by a vibrating two-sided perfect mirror. The Hamiltonian of the system is obtained starting from its canonical quantisation, as shown in Methods, and it accounts also for generic equilibrium positions of the mirror. Our main result is the discovery of a photon-pair hopping mechanism, in a coherent second-order ef-

fective resonant dynamics.

This effect has been described analytically through the generalized James' approach (see Methods) under the condition $\omega_a = \omega_c$. The numerical analysis of the lowest energy levels showed an avoided-level crossing around the resonant condition [see Fig. 2(c)]. This gap is a trademark of the hybridisation of two photon-pair states. We have performed a stochastic evolution of the system wave function (see Methods) in which we witnessed a coherent oscillatory dynamics between the states $|2, 0, 0\rangle$ and $|0, 0, 2\rangle$.

The effects described here could be experimentally reproduced, with the chosen parameters, in circuit-optomechanical systems by using ultra-high-frequency mechanical micro- or nano-resonators in the GHz spectral range; alternatively, using two *LC* circuits bridged by a SQUID. Moreover, in arrays of non-linearly coupled cavities [52], where the photon crystal associated to a periodic modulation of the photon blockade can emerge, the optomechanical system proposed here allows investigating a new mechanism of photon-pair propagation in optomechanical lattices [53, 54].

METHODS

Derivation of the system Hamiltonian. We begin by considering two non-interacting electromagnetic cavities separated by a perfect movable mirror. For simplicity, following Ref. [46], we conduct our analysis in *1D* and generalise it to our case. To set the notation, $\pm I$ denotes the extremes of the cavity, M and $q(t)$ the mass and the position of the movable mirror respectively. The electromagnetic field, in absence of charges, obeys the wave equation; the motion of the movable mirror is influenced by the radiation pressure of the fields in the two cavities [see Fig. 2(a) in the main text], so that, it satisfies the Newton's equation

$$\begin{cases} \Delta A = 0 & x \in (-I, q) \cup (q, I) \\ M\ddot{q} = -\partial_q V + \frac{1}{2} [(\partial_- A)^2 - (\partial_+ A)^2]|_q \end{cases} \quad (7)$$

where $\Delta := \partial_t^2 - \partial_x^2$ and ∂_-, ∂_+ are the left and right derivatives. The potential $V(q)$ is designed to have infinite walls at the two mirror positions $\pm I$. The two radiation pressures $(\partial_{\pm} A)^2/2$ come with opposite signs and in the form of lateral derivatives, because of the negligible thickness of the movable mirror.

By defining L_k and R_k as the Fourier components on the left and right cavity, respectively, the completeness of the mode functions enables to write

$$A(t, x) = \begin{cases} L^k(t) \varphi_k(t, x) & x \in (-I, q) \\ R^k(t) \phi_k(t, x) & x \in (q, I) \end{cases} \quad (8)$$

where the summation in k is understood and

$$\begin{aligned}\varphi_k &= \sqrt{\frac{2}{q+I}} \sin[\omega_k(x+I)], \\ \phi_k &= \sqrt{\frac{2}{I-q}} \sin[\Omega_k(x-I)],\end{aligned}\quad (9)$$

with $\omega_k = k\pi/(q+I)$, $\Omega_k = k\pi/(I-q)$. We can still fix a normalisation for φ_k and ϕ_k choosing

$$\delta_{ij} = \int_{-I}^q \varphi_i \varphi_j = \int_q^I \phi_i \phi_j, \quad (10)$$

as the Kronecker delta. The wave equation Eq. (7) can be projected along one Fourier component, and the equation of motion of the movable mirror becomes

$$\begin{aligned}\ddot{L}_k + \omega_k^2 L_k - \frac{g_{km} (2\dot{q}\dot{L}^m + \ddot{q}L^m)}{I+q} \\ + \dot{q}^2 \frac{(g_{km} + g_{kj}g^j_m) L^m}{(I+q)^2} = 0, \\ \ddot{R}_k + \Omega_k^2 R_k - \frac{\gamma_{km} (2\dot{q}\dot{R}^m + \ddot{q}R^m)}{I-q} \\ - \dot{q}^2 \frac{(\gamma_{km} - \gamma_{kj}\gamma^j_m) R^m}{(I-q)^2} = 0, \\ M\ddot{q} + \partial_q V + (-1)^{k+m} \left(\frac{\Omega_k \Omega_m R^k R^m}{I-q} - \frac{\omega_k \omega_m L^k L^m}{q+I} \right) = 0,\end{aligned}\quad (11)$$

with

$$\begin{aligned}g_{km} &= (q+I) \int_{-I}^q \partial_q(\varphi_k) \varphi_m \\ &= -\gamma_{km} = -(I-q) \int_q^I \partial_q(\phi_k) \phi_m,\end{aligned}\quad (12)$$

that satisfy

$$\begin{aligned}g_{kj}g^j_m &= -(q+I)^2 \int_{-I}^q \partial_q \varphi_k \partial_q \varphi_m \\ &= \gamma_{kj}\gamma^j_m = -(I-q)^2 \int_q^I \partial_q \phi_k \partial_q \phi_m,\end{aligned}\quad (13)$$

and

$$\begin{aligned}\int_{-I}^q \varphi_k \partial_q^2 \varphi_m &= \frac{1}{(q+I)^2} (g_{kj}g^j_m - g_{km}), \\ \int_q^I \phi_k \partial_q^2 \phi_m &= \frac{1}{(I-q)^2} (\gamma_{kj}\gamma^j_m + \gamma_{km}).\end{aligned}\quad (14)$$

The system of equations Eq. (7) can be derived from the following Lagrangian

$$\begin{aligned}\mathcal{L}(q, \dot{q}, L, \dot{L}, R, \dot{R}) = \\ \frac{1}{2} (\dot{L}_k \dot{L}^k - \omega_k^2 L_k L^k + \dot{R}_k \dot{R}^k - \Omega_k^2 R_k R^k) \\ + \frac{1}{2} M \dot{q}^2 - V - \dot{q} \left(g_{km} \frac{\dot{L}^k L^m}{q+I} + \gamma_{km} \frac{\dot{R}^k R^m}{I-q} \right) \\ - \frac{\dot{q}^2}{2} \left[g_{kj}g^j_m \frac{L^k L^m}{(q+I)^2} + \gamma_{kj}\gamma^j_m \frac{R^k R^m}{(I-q)^2} \right],\end{aligned}\quad (15)$$

and the corresponding Hamiltonian is

$$\begin{aligned}\mathcal{H}(q, p, L, \Lambda, R, W) = \\ \frac{1}{2M} \left(p + g_{km} \frac{\Lambda^k L^m}{q+I} + \gamma_{km} \frac{W^k R^m}{I-q} \right)^2 + V \\ + \frac{1}{2} (\Lambda_k \Lambda^k + \omega_k^2 L^k L^k) + \frac{1}{2} (W_k W^k + \Omega_k^2 R^k R^k).\end{aligned}\quad (16)$$

To quantise the Hamiltonian, consider the operators $\{\hat{q}, \hat{p}, \hat{L}_k, \hat{\Lambda}_k, \hat{R}_k, \hat{W}_k\}$ and impose the commutation relations ($\hbar = 1$), $[\hat{q}, \hat{p}] = i$, $[\hat{L}_k, \hat{\Lambda}_m] = i\delta_{km}$ and $[\hat{R}_k, \hat{W}_m] = i\delta_{km}$, while $[\hat{q}, \hat{L}_m] = [\hat{q}, \hat{R}_m] = [\hat{L}_k, \hat{R}_m] = [\hat{p}, \hat{L}_m] = [\hat{p}, \hat{W}_m] = [\hat{\Lambda}_k, \hat{W}_m] = 0$. Using the ladder operators

$$\begin{aligned}\hat{a}_k &= \frac{1}{\sqrt{2\omega_k}} (\omega_k \hat{L}_k + i\hat{\Lambda}_k), \\ \hat{c}_k &= \frac{1}{\sqrt{2\Omega_k}} (\Omega_k \hat{R}_k + i\hat{W}_k),\end{aligned}\quad (17)$$

the Hamiltonian Eq. (16) becomes

$$\begin{aligned}\hat{H}' = \frac{(\hat{p} + \hat{\Gamma})^2}{2M} + \hat{V} + \sum_k \omega_k \hat{a}_k^\dagger \hat{a}_k \\ + \sum_k \Omega_k \hat{c}_k^\dagger \hat{c}_k - \frac{\pi q}{6(q+I)(q-I)} \mathbb{1},\end{aligned}\quad (18)$$

where we have already resummed the vacuum point fluctuations, and

$$\begin{aligned}\hat{\Gamma} = \frac{i}{2} \sqrt{\frac{m}{k}} \left[\frac{g^{km} (\hat{a}_k^\dagger - \hat{a}_k) (\hat{a}_m^\dagger + \hat{a}_m)}{q+I} \right. \\ \left. + \frac{\gamma^{km} (\hat{c}_k^\dagger - \hat{c}_k) (\hat{c}_m^\dagger + \hat{c}_m)}{I-q} \right].\end{aligned}\quad (19)$$

This is the full Hamiltonian of the problem. In order to derive Eq. (1) we still need to linearise it and consider the unimodal case. To linearise, first consider $\Gamma \approx \Gamma_0$ constant and then introduce a variation from the expected position of the mirror $q = q_0 + \delta q$, and expand all the terms accordingly

$$\begin{aligned}\omega_k &= \frac{k\pi}{q_0+I} \left(1 - \frac{\delta q}{q_0+I} \right) + \mathcal{O} \left[\frac{\delta q^2}{(q_0+I)^2} \right], \\ \Omega_k &= \frac{k\pi}{I-q_0} \left(1 + \frac{\delta q}{I-q_0} \right) + \mathcal{O} \left[\frac{\delta q^2}{(I-q_0)^2} \right],\end{aligned}\quad (20)$$

which in turn, from Eq. (17), induces

$$\begin{aligned}\hat{a}_k &\approx (\hat{a}_0)_k - \frac{\delta q}{2(q_0+I)} (\hat{a}_0^\dagger)_k, \\ \hat{c}_k &\approx (\hat{c}_0)_k + \frac{\delta q}{2(I-q_0)} (\hat{c}_0^\dagger)_k.\end{aligned}\quad (21)$$

Performing the unitary transformation $\hat{U} = \exp(i\delta q \hat{\Gamma}_0)$ on Eq. (18), proves that

$$\begin{aligned} \hat{H} &= \hat{U} \hat{H}' \hat{U}^\dagger = \frac{\hat{p}^2}{2M} + \hat{V} \\ &+ \sum_k \left[(\omega_0)_k (\hat{a}_0^\dagger)_k (\hat{a}_0)_k + (\Omega_0)_k (\hat{c}_0^\dagger)_k (\hat{c}_0)_k \right] \\ &- \delta q (\hat{G}_0 + \hat{F}_0), \end{aligned} \quad (22)$$

where $\hat{V} = \hat{V} - \pi q \hat{\mathbb{1}}/6(q+I)(q-I)$ and

$$\begin{aligned} \hat{F}_0 &= \frac{1}{2(q_0+I)} \sum_{k,j} (-1)^{k+j} \sqrt{(\omega_k \omega_j)_0} (\hat{a}_k^\dagger + \hat{a}_k) (\hat{a}_m^\dagger + \hat{a}_m), \\ \hat{G}_0 &= -\frac{1}{2(I-q_0)} \sum_{k,j} (-1)^{k+j} \sqrt{(\Omega_k \Omega_j)_0} (\hat{c}_k^\dagger + \hat{c}_k) (\hat{c}_m^\dagger + \hat{c}_m). \end{aligned} \quad (23)$$

To finally obtain Eq. (1) in the main text, we consider a quadratic potential V and introduce the vibrating mirror ladder operators $\{b, b^\dagger\}$ in a way that $\delta q = x_{\text{zpf}}(b + b^\dagger)$, where x_{zpf} is the zero-point-fluctuation amplitude of the vibrating mirror. By reducing all the modes to one ($k = j = 1$), the system Hamiltonian in Eq. (18) can be written down as

$$\begin{aligned} \hat{H} &= \omega_a \hat{a}^\dagger \hat{a} + \omega_b \hat{b}^\dagger \hat{b} + \omega_c \hat{c}^\dagger \hat{c} \\ &+ \frac{x_{\text{zpf}}}{2\pi} [\omega_c^2 (\hat{c} + \hat{c}^\dagger)^2 - \omega_a^2 (\hat{a} + \hat{a}^\dagger)^2] (\hat{b} + \hat{b}^\dagger). \end{aligned} \quad (24)$$

Defining a coupling strength $g = \omega_c^2 x_{\text{zpf}}/\pi = \omega_c x_{\text{zpf}}/(I - q_0)$ the Eq. (1) in the main text is obtained. Note that since $\hbar = 1$ the coupling strength g has the right units.

Derivation of the effective Hamiltonians: Applying the generalized James' method. For interacting quantum systems that are strongly detuned, an effective Hamiltonian can be derived using the generalized James' effective Hamiltonian method [49]. To apply this method to Eq. (1), we first rewrite it in the interaction picture,

$$\begin{aligned} \hat{H}_1(t) &= g \left[\hat{c}^\dagger \hat{c} - \frac{\omega_a^2}{\omega_c^2} \hat{a}^\dagger \hat{a} \right] \hat{b} e^{-i\omega_b t} \\ &+ \frac{g}{2} \left[(\hat{c})^2 \hat{b} e^{-i(\omega_b + 2\omega_c)t} - \frac{\omega_a^2}{\omega_c^2} (\hat{a})^2 \hat{b} e^{-i(\omega_b + 2\omega_a)t} \right] \\ &+ \frac{g}{2} \left[(\hat{c}^\dagger)^2 \hat{b} e^{i(2\omega_c - \omega_b)t} - \frac{\omega_a^2}{\omega_c^2} (\hat{a}^\dagger)^2 \hat{b} e^{i(2\omega_a - \omega_b)t} \right] \\ &+ \text{h.c.} \end{aligned} \quad (25)$$

This can be rewritten as

$$\hat{H}_1(t) = \sum_k \left[\hat{h}_k e^{-i\omega_k t} + \hat{h}_k^\dagger e^{i\omega_k t} \right]. \quad (26)$$

where now the ω_k are a combination of the bare transition frequencies. It turns out that, a photon-pairs hopping

mechanism already appears with a second-order generalized James' effective Hamiltonian method [49]. This accounts for calculating

$$\hat{H}_1^{(2)}(t) = \sum_{j,k} \frac{1}{\omega_k} \left[\hat{h}_j \hat{h}_k^\dagger e^{i(\omega_k - \omega_j)t} - \hat{h}_j^\dagger \hat{h}_k e^{i(\omega_j - \omega_k)t} \right]. \quad (27)$$

In the rotating-wave approximation, all frequency contributions which are different from zero can be neglected. Since the frequencies ω_k are all different, we only keep the terms in $\hat{H}_1^{(2)}(t)$ where the sum of the exponent is zero.

Starting from Eq. (25) and considering the resonant condition $\omega_a = \omega_c$, only three terms need to be considered

$$\begin{aligned} \hat{h}_1 &= \frac{g}{2} (\hat{c}^{\dagger 2} - \hat{a}^{\dagger 2}) \hat{b}^\dagger & \omega_1 &= 2\omega_a + \omega_b, \\ \hat{h}_2 &= \frac{g}{2} (\hat{c}^{\dagger 2} - \hat{a}^{\dagger 2}) \hat{b} & \omega_2 &= 2\omega_a - \omega_b, \\ \hat{h}_3 &= \frac{g}{2} (\{\hat{c}, \hat{c}^\dagger\} - \{\hat{a}, \hat{a}^\dagger\}) \hat{b}^\dagger & \omega_3 &= \omega_b. \end{aligned} \quad (28)$$

From the canonical commutation relations it follows that

$$\begin{aligned} [\hat{h}_1, \hat{h}_1^\dagger] &= \frac{g^2}{4} \left[\hat{a}^2 \hat{c}^{\dagger 2} + \hat{a}^{\dagger 2} \hat{c}^2 - \hat{c}^{\dagger 2} \hat{c}^2 - \hat{a}^{\dagger 2} \hat{a}^2 \right. \\ &\quad \left. + 2\hat{b}^\dagger \hat{b} (\{\hat{c}, \hat{c}^\dagger\} + \{\hat{a}, \hat{a}^\dagger\}) \right], \\ [\hat{h}_2, \hat{h}_2^\dagger] &= \frac{g^2}{4} \left[\hat{c}^{\dagger 2} \hat{c}^2 + \hat{a}^{\dagger 2} \hat{a}^2 - \hat{c}^{\dagger 2} \hat{a}^2 - \hat{a}^{\dagger 2} \hat{c}^2 \right. \\ &\quad \left. + 2\hat{b} \hat{b}^\dagger (\{\hat{c}, \hat{c}^\dagger\} + \{\hat{a}, \hat{a}^\dagger\}) \right], \\ [\hat{h}_3, \hat{h}_3^\dagger] &= -g^2 (\hat{c}^\dagger \hat{c} - \hat{a}^\dagger \hat{a})^2, \end{aligned}$$

so James' effective Hamiltonian is

$$\begin{aligned} \hat{H}_{\text{eff}}^{(2)} &= \left[\omega_a + \frac{g^2(4\omega_a + \omega_b)}{8\omega_a^2 - 2\omega_b^2} \right] (\hat{c}^\dagger \hat{c} + \hat{a}^\dagger \hat{a}) \\ &+ \frac{g^2(3\omega_b^2 - 8\omega_a^2)}{(8\omega_a^2 - 2\omega_b^2)\omega_b} [(\hat{c}^\dagger \hat{c})^2 + (\hat{a}^\dagger \hat{a})^2] \\ &+ \left[\omega_b + \frac{4g^2\omega_a}{4\omega_a^2 - \omega_b^2} (\hat{c}^\dagger \hat{c} + \hat{a}^\dagger \hat{a} + \mathbb{1}) \right] \hat{b}^\dagger \hat{b} \\ &+ \frac{2g^2}{\omega_b} \hat{a}^\dagger \hat{a} \hat{c}^\dagger \hat{c} + \frac{g^2}{2\omega_a - \omega_b} \mathbb{1} \\ &- \frac{g^2\omega_b}{8\omega_a^2 - 2\omega_b^2} (\hat{a}^2 \hat{c}^{\dagger 2} + \hat{a}^{\dagger 2} \hat{c}^2). \end{aligned} \quad (29)$$

All the terms but the last one are energy shifts. The latter is the desired hopping mechanism.

Monte Carlo wave function approach: Quantum trajectory. Following Refs. [55, 56], in order to describe the Monte Carlo wave function (MCWF) approach, we introduce the non-Hermitian Hamiltonian

$$\hat{\mathcal{H}} = \hat{H} - \frac{i}{2} \sum_m \gamma_m \hat{\Gamma}_m^\dagger \hat{\Gamma}_m, \quad (30)$$

describing the effect of the environment between two quantum jumps. Here, \hat{H} represents the Hamiltonian part of the dynamics, and one can either use the full or the effective Hamiltonian, while $\hat{\Gamma}_m$ are the jump operators. The evolution of a quantum trajectory is thus dictated by a non-Hermitian evolution via $\hat{\mathcal{H}}$ interrupted by random quantum jumps. The algorithm to obtain such a dynamics reads:

- (i) $|\psi(t)\rangle$ is the normalized wave function at the initial time t .
- (ii) The probability that a quantum jump occurs through the m -th dissipative channel in a small amount of time dt is

$$\delta p_m(t) = dt \gamma_m \langle \psi(t) | \hat{\Gamma}_m^\dagger \hat{\Gamma}_m | \psi(t) \rangle, \quad (31)$$

such that $\delta p_m(t) \ll 1$.

- (iii) One randomly generates a real number $\varepsilon \in [0, 1]$.
- (iv) If $\sum_m \delta p_m(t) < \varepsilon$, no quantum jump occurs, and

the system evolves as

$$|\psi(t+dt)\rangle = \exp(-i\hat{\mathcal{H}}dt) = \mathbb{1} - idt\hat{\mathcal{H}}|\psi(t)\rangle + \mathcal{O}(dt^2). \quad (32)$$

- (v) Otherwise, if $\sum_m \delta p_m(t) > \varepsilon$, a quantum jump occurs. To decide which channel dissipates, a second random number ε' is generated, and each quantum jump is selected with probability $\delta p_m(t)/(\sum_n \delta p_n(t))$. The wave function then becomes

$$|\psi(t+dt)\rangle = \hat{\Gamma}_m |\psi(t)\rangle. \quad (33)$$

- (vi) At this point, independently of whether a quantum jump took place, the wave function $|\psi(t+dt)\rangle$ is renormalized and used for the next step of the time evolution.

Any quantum jump corresponds to the projection of the wave function associated with a generalized measurement process (wave-function collapse through a positive operator-valued measure) [57]. Although the results of MCWF recovers those of the Lindblad master equation, by averaging over an infinite number of trajectories, noise effects determine the convergence rate.

-
- [1] W. Marshall, C. Simon, R. Penrose, and D. Bouwmeester, Towards quantum superpositions of a mirror, *Phys. Rev. Lett.* **91**, 130401 (2003).
 - [2] E. Gavartin, P. Verlot, and T. J. Kippenberg, A hybrid on-chip optomechanical transducer for ultrasensitive force measurements, *Nature Nanotechnology* **7**, 509 (2012).
 - [3] J. D. Teufel, T. Donner, M. A. Castellanos-Beltran, J. W. Harlow, and K. W. Lehnert, Nanomechanical motion measured with an imprecision below that at the standard quantum limit, *Nature Nanotechnology* **4**, 820 (2009).
 - [4] A. G. Krause, M. Winger, T. D. Blasius, Q. Lin, and O. Painter, A high-resolution microchip optomechanical accelerometer, *Nature Photonics* **6**, 768 (2012).
 - [5] M. Carlesso and M. Paternostro, Opto-mechanical test of collapse models, in *Do Wave Functions Jump? : Perspectives of the Work of GianCarlo Ghirardi*, edited by V. Allori, A. Bassi, D. Dürr, and N. Zanghi (Springer International Publishing, Cham, 2021) pp. 205–215.
 - [6] G. Anetsberger, O. Arcizet, Q. P. Unterreithmeier, R. Rivière, A. Schliesser, E. M. Weig, J. P. Kotthaus, and T. J. Kippenberg, Near-field cavity optomechanics with nanomechanical oscillators, *Nature Physics* **5**, 909 (2009).
 - [7] P. Verlot, A. Tavernarakis, T. Briant, P.-F. Cohadon, and A. Heidmann, Scheme to probe optomechanical correlations between two optical beams down to the quantum level, *Phys. Rev. Lett.* **102**, 103601 (2009).
 - [8] S. Barzanjeh, A. Xuereb, S. Gröblacher, M. Paternostro, C. A. Regal, and E. M. Weig, Optomechanics for quantum technologies, *Nature Physics* **18**, 15 (2022).
 - [9] A. Schliesser, O. Arcizet, R. Rivière, G. Anetsberger, and T. J. Kippenberg, Resolved-sideband cooling and position measurement of a micromechanical oscillator close to the Heisenberg uncertainty limit, *Nature Physics* **5**, 509 (2009).
 - [10] S. Gröblacher, J. B. Hertzberg, M. R. Vanner, G. D. Cole, S. Gigan, K. C. Schwab, and M. Aspelmeyer, Demonstration of an ultracold micro-optomechanical oscillator in a cryogenic cavity, *Nature Physics* **5**, 485 (2009).
 - [11] J. D. Teufel, T. Donner, D. Li, J. W. Harlow, M. S. Allman, K. Cicak, A. J. Sirois, J. D. Whittaker, K. W. Lehnert, and R. W. Simmonds, Sideband cooling of micromechanical motion to the quantum ground state, *Nature* **475**, 359 (2011).
 - [12] I. Wilson-Rae, N. Nooshi, W. Zwerger, and T. J. Kippenberg, Theory of ground state cooling of a mechanical oscillator using dynamical backaction, *Phys. Rev. Lett.* **99**, 093901 (2007).
 - [13] J. Chan, T. P. M. Alegre, A. H. Safavi-Naeini, J. T. Hill, A. Krause, S. Gröblacher, M. Aspelmeyer, and O. Painter, Laser cooling of a nanomechanical oscillator into its quantum ground state, *Nature* **478**, 89 (2011).
 - [14] T. Ojanen and K. Børkje, Ground-state cooling of mechanical motion in the unresolved sideband regime by use of optomechanically induced transparency, *Phys. Rev. A* **90**, 013824 (2014).
 - [15] K. Stannigel, P. Komar, S. J. M. Habraken, S. D. Bennett, M. D. Lukin, P. Zoller, and P. Rabl, Optomechanical quantum information processing with photons and phonons, *Phys. Rev. Lett.* **109**, 013603 (2012).
 - [16] L. Garziano, R. Stassi, V. Macrì, S. Savasta, and O. Di Stefano, Single-step arbitrary control of mechanical quantum states in ultrastrong optomechanics, *Phys. Rev. A* **91**, 023809 (2015).
 - [17] P. Meystre, A short walk through quantum optomechanics, *Annalen der Physik* **525**, 215 (2013).
 - [18] V. Macrì, L. Garziano, A. Ridolfo, O. Di Stefano, and

- S. Savasta, Deterministic synthesis of mechanical noon states in ultrastrong optomechanics, *Phys. Rev. A* **94**, 013817 (2016).
- [19] M. Eichenfield, R. Camacho, J. Chan, K. J. Vahala, and O. Painter, A picogram- and nanometre-scale photonic-crystal optomechanical cavity, *Nature* **459**, 550 (2009).
- [20] M. Eichenfield, J. Chan, R. M. Camacho, K. J. Vahala, and O. Painter, Optomechanical crystals, *Nature* **462**, 78 (2009).
- [21] X. Zhang, T. Lin, F. Tian, H. Du, Y. Zou, F. S. Chau, and G. Zhou, Mode competition and hopping in optomechanical nano-oscillators, *Applied Physics Letters* **112**, 153502 (2018).
- [22] D. Chang, A. H. Safavi-Naeini, M. Hafezi, and O. Painter, Slowing and stopping light using an optomechanical crystal array, *New J. Phys.* **13**, 023003 (2011).
- [23] M. Schmidt, M. Ludwig, and F. Marquardt, Optomechanical circuits for nanomechanical continuous variable quantum state processing, *New J. Phys.* **14**, 125005 (2012).
- [24] M. Aspelmeyer, T. J. Kippenberg, and F. Marquardt, Cavity optomechanics, *Rev. Mod. Phys.* **86**, 1391 (2014).
- [25] F. Y. Khalili and S. L. Danilishin, Quantum optomechanics, *Progress in Optics* **61**, 113 (2016).
- [26] A. D. O'Connell, M. Hofheinz, M. Ansmann, R. C. Bialczak, M. Lenander, E. Lucero, M. Neeley, D. Sank, H. Wang, M. Weides, J. Wenner, J. M. Martinis, and A. N. Cleland, Quantum ground state and single-phonon control of a mechanical resonator, *Nature* **464**, 697 (2010).
- [27] F. Rouxinol, Y. Hao, F. Brito, A. Caldeira, E. Irish, and M. LaHaye, Measurements of nanoresonator-qubit interactions in a hybrid quantum electromechanical system, *Nanotechnology* **27**, 364003 (2016).
- [28] G. T. Moore, Quantum theory of the electromagnetic field in a variable-length one-dimensional cavity, *J. Math. Phys.* **11**, 2679 (1970).
- [29] P. D. Nation, J. R. Johansson, M. P. Blencowe, and F. Nori, Stimulating uncertainty: Amplifying the quantum vacuum with superconducting circuits, *Rev. Mod. Phys.* **84**, 1 (2012).
- [30] J. R. Johansson, G. Johansson, C. Wilson, and F. Nori, Dynamical Casimir effect in a superconducting coplanar waveguide, *Phys. Rev. Lett.* **103**, 147003 (2009).
- [31] J. R. Johansson, G. Johansson, C. M. Wilson, and F. Nori, Dynamical Casimir effect in superconducting microwave circuits, *Phys. Rev. A* **82**, 052509 (2010).
- [32] C. Wilson, G. Johansson, A. Pourkabirian, M. Simoen, J. Johansson, T. Duty, F. Nori, and P. Delsing, Observation of the dynamical Casimir effect in a superconducting circuit, *Nature* **479**, 376 (2011).
- [33] V. Dodonov, Fifty years of the dynamical Casimir effect, *Physics* **2**, 67 (2020).
- [34] V. Macrì, A. Ridolfo, O. Di Stefano, A. F. Kockum, F. Nori, and S. Savasta, Nonperturbative dynamical Casimir effect in optomechanical systems: Vacuum Casimir-Rabi splittings, *Phys. Rev. X* **8**, 011031 (2018).
- [35] A. Settinieri, V. Macrì, A. Ridolfo, O. Di Stefano, A. F. Kockum, F. Nori, and S. Savasta, Dissipation and thermal noise in hybrid quantum systems in the ultrastrong-coupling regime, *Phys. Rev. A* **98**, 053834 (2018).
- [36] A. Settinieri, V. Macrì, L. Garziano, O. Di Stefano, F. Nori, and S. Savasta, Conversion of mechanical noise into correlated photon pairs: Dynamical Casimir effect from an incoherent mechanical drive, *Phys. Rev. A* **100**, 022501 (2019).
- [37] K. Y. Fong, H.-K. Li, R. Zhao, S. Yang, Y. Wang, and X. Zhang, Phonon heat transfer across a vacuum through quantum fluctuations, *Nature* **576**, 243 (2019).
- [38] S. Butera and I. Carusotto, Mechanical backreaction effect of the dynamical Casimir emission, *Phys. Rev. A* **99**, 053815 (2019).
- [39] A. Ferreri, H. Pfeifer, F. K. Wilhelm, S. Hofferberth, and D. E. Bruschi, On the interplay between optomechanics and the dynamical Casimir effect, *arXiv preprint arXiv:2204.10724* (2022).
- [40] O. Di Stefano, A. Settinieri, V. Macrì, A. Ridolfo, R. Stassi, A. F. Kockum, S. Savasta, and F. Nori, Interaction of mechanical oscillators mediated by the exchange of virtual photon pairs, *Phys. Rev. Lett.* **122**, 030402 (2019).
- [41] S. Butera, Influence functional for two mirrors interacting via radiation pressure, *Phys. Rev. D* **105**, 016023 (2022).
- [42] T. T. Heikkilä, F. Massel, J. Tuorila, R. Khan, and M. A. Sillanpää, Enhancing optomechanical coupling via the Josephson effect, *Phys. Rev. Lett.* **112**, 203603 (2014).
- [43] J. Pirkkalainen, S. Cho, F. Massel, J. Tuorila, T. Heikkilä, P. Hakonen, and M. Sillanpää, Cavity optomechanics mediated by a quantum two-level system, *Nat. Commun.* **6**, 1 (2015).
- [44] J. R. Johansson, G. Johansson, and F. Nori, Optomechanical-like coupling between superconducting resonators, *Phys. Rev. A* **90**, 053833 (2014).
- [45] E.-j. Kim, J. R. Johansson, and F. Nori, Circuit analog of quadratic optomechanics, *Phys. Rev. A* **91**, 033835 (2015).
- [46] C. K. Law, Interaction between a moving mirror and radiation pressure: A Hamiltonian formulation, *Phys. Rev. A* **51**, 2537 (1995).
- [47] F. Montalbano, F. Armata, L. Rizzuto, and R. Passante, Spatial correlations of field observables in two half-spaces separated by a movable perfect mirror, *arXiv preprint arXiv:2204.06886* (2022).
- [48] H. K. Cheung and C. K. Law, Nonadiabatic optomechanical Hamiltonian of a moving dielectric membrane in a cavity, *Phys. Rev. A* **84**, 023812 (2011).
- [49] W. Shao, C. Wu, and X. Feng, Generalized James' effective Hamiltonian method, *Phys. Rev. A* **95**, 032124 (2017).
- [50] F. Minganti, V. Macrì, A. Settinieri, S. Savasta, and F. Nori, Dissipative state transfer and Maxwell's demon in single quantum trajectories: Excitation transfer between two noninteracting qubits via unbalanced dissipation rates, *Phys. Rev. A* **103**, 052201 (2021).
- [51] V. Macrì, F. Minganti, A. F. Kockum, A. Ridolfo, S. Savasta, and F. Nori, Revealing higher-order light and matter energy exchanges using quantum trajectories in ultrastrong coupling, *Phys. Rev. A* **105**, 023720 (2022).
- [52] J. Jin, D. Rossini, R. Fazio, M. Leib, and M. J. Hartmann, Photon solid phases in driven arrays of nonlinearly coupled cavities, *Phys. Rev. Lett.* **110**, 163605 (2013).
- [53] W. Chen and A. A. Clerk, Photon propagation in a one-dimensional optomechanical lattice, *Phys. Rev. A* **89**, 033854 (2014).
- [54] M. Schmidt, S. Kessler, V. Peano, O. Painter, and F. Marquardt, Optomechanical creation of magnetic fields for photons on a lattice, *Optica* **2**, 635 (2015).
- [55] J. Dalibard, Y. Castin, and K. Mølmer, Wave-function

approach to dissipative processes in quantum optics, *Phys. Rev. Lett.* **68**, 580. (1992).

- [56] K. Mølmer, Y. Castin, and J. Dalibard, Monte Carlo wave-function method in quantum optics, *J. Opt. Soc. Am. B* **10**, 524 (1993).
- [57] H. Wiseman and G. Milburn, *Quantum Measurement and Control* (Cambridge University Press, Cambridge, 2010).

Acknowledgements

F.N. is supported in part by: Nippon Telegraph and Telephone Corporation (NTT) Research, the Japan Science and Technology Agency (JST) [via the Quantum

Leap Flagship Program (Q-LEAP), and the Moonshot R&D Grant Number JPMJMS2061], the Japan Society for the Promotion of Science (JSPS) [via the Grants-in-Aid for Scientific Research (KAKENHI) Grant No. JP20H00134], the Army Research Office (ARO) (Grant No. W911NF-18-1-0358), the Asian Office of Aerospace Research and Development (AOARD) (via Grant No. FA2386-20-1-4069), and the Foundational Questions Institute Fund (FQXi) via Grant No. FQXi-IAF19-06. S.S. acknowledges the Army Research Office (ARO) (Grant No. W911NF-19-1-0065). R.L.F. is supported by European Union (Next Generation EU) via MUR D.M. Grant No. 737-2021.